Environmental Effects upon Fatigue and Fracture Propagation of A1N Grade Railway Steel

S. Beretta[1, a], M. Carboni[1,b] A. Lo Conte[1,c]

[1]Politecnico di Milano, Department of Mechanical Engineering, via La Masa 34, Milano, Italy.

[a]stefano.beretta@polimi.it, [b]michele.carboni@polimi.it, [c]antonietta.loconte@polimi.it

Keywords: A1N steel, railway axles, corrosion pits, fatigue-corrosion.

Abstract. The European approach to the design and manufacturing of railway axles does not provide unified criteria to interpret the effects of track behaviour, corrosion protection quality, suspension performance and maintenance practice. In the present paper, the S-N curve in corrosive environment has been experimentally derived observing failures also in the super-long fatigue regime. The pit-to-crack transition has then been analysed. Moreover, crack propagations tests have been carried out in both laboratory air and corrosive environment on SE(B) specimens by means of a dedicated bench in order to analyse the influence of corrosion upon crack rates of A1N steel railway axles.

Introduction

Increasing attention is being paid to the analysis of fatigue properties [1, 2] and crack growth in railway axles [3] in order to better define fatigue design [4] and the scheduling of inspection for these components.

The effects of corrosion on fatigue properties can firstly be observed as a number of surface defects or pits which obviously reduce the fatigue strength of the axle body [5, 6], whereas in general "corrosion fatigue" detrimentally influences both crack initiation and crack growth [7]. This phenomenon is characterised by the formation of a consistent number of small cracks, whose nucleation is favoured by the pits due to the aggressive environment. These small cracks are then able to cross the microstructural barriers [8-9] with ease and a much faster growth rate than in air. These effects result in a large decrease in fatigue properties even in gentle environments with a disappearing of the "knee" of the S-N diagram. Previous research has provided some clues/indications as to the fatigue properties of carbon steels: i) rotating bending fatigue tests by Endo and Miyao of a mild carbon (reported by Schjive [7]) steel in tap water showed a reduction of fatigue strength of the order of 50%; ii) fatigue tests in tap water for an AISI 1018 steel showed fatigue strengths of 120 MPa at 2×10^6 cycles (approx. 50% of fatigue limit in air) and 90 MPa at 10^7 cycles [10].

This experimental evidence shows a detrimental effect of the environment upon the S-N diagram which can be taken into account applying a reduction of the fatigue design limit [11-12] or by means of particular requirements for corrosion protection levels [15, 16].

In recent papers, the assessment of the high cycle fatigue strength, in presence of corrosion pits, of axles produced in A1N steel has been investigated by the authors based on a detailed statistical analysis of the maximum dimension of defects carried out on samplings taken form axles retired from service [17, 18]. In the present paper, a series of axial fatigue tests, in air and in corrosive environment on smooth and micro-notched cylindrical specimens, is presented. The S-N data for complete failure of the specimen have been obtained and the pit-to-crack transition has then been analysed. Moreover, crack propagation tests have been carried out in both laboratory air and corrosive environment on SE(B) specimens by means of a dedicated bench in order to analyse the influence of corrosion upon crack rates of A1N steel railway axles.

Experiments in laboratory air

Basic mechanical behaviour A1N mild carbon steel is widely used for manufacturing railway axles [19]. Basic mechanical properties are [20]: ultimate tensile strength UTS=597 MPa, monotonic yield strength $\sigma_{y,monotonic}$=395 MPa. Cyclic properties are: 0.2% cyclic proof stress $\sigma_{y,cyc0.2}$=357 MPa, 0.05% cyclic proof stress $\sigma_{y,cyc0.05}$=289 MPa. Parameters of the cyclic Ramberg-Osgood relationship are equal to E_{cyc}=209303 MPa, n=0.150395 and H=907.34 MPa.

Fatigue limit tests Various series of fatigue tests were carried out in order to determine the Kitagawa-Takahashi diagram [21], i.e. the relationship between fatigue limit and crack size, for the A1N steel at R=-1.

Four different sets of fatigue limit tests were carried out: one series on smooth specimens and three other series on micro-notched specimens. All the specimens were hourglass shaped with a minimum diameter of 10 mm (Fig. 1a). After machining, the specimens were hand polished up to #1000 grit emery paper and then electro-polished (94% acetic and 6% perchloric acid solution) in order to remove a 30 μm layer. Three series of specimens were machined by EDM in order to obtain narrow surface micro-notches (Fig. 1b) with respective dimensions of 200×100 μm (√area=140 μm), 500×100 μm (√area=224 μm) and 2000×200 μm (√area=632 μm). Fatigue tests were carried out under axial loading (R=-1) conditions by a RUMUL Testronic® resonance testing machine (maximum nominal load equal to 100 kN) working at a frequency of approximately 90 Hz. "Stair-case" sequences were applied: specimens were considered "run-outs" if they survived 12×10^6 cycles.

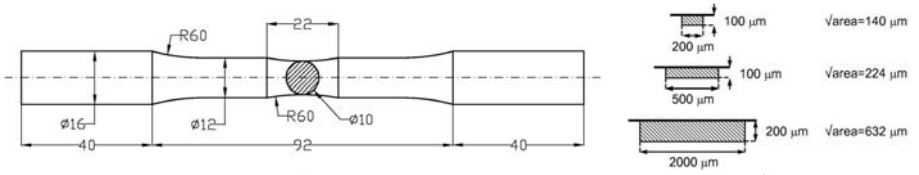

(a) (b)

Fig. 1: Fatigue experiments in air (R=-1): a) geometry of adopted specimens; b) dimensions of adopted artificial micro-notches.

Experimental results are reported in Fig. 2a in terms of fatigue limit stress amplitudes σ_w corresponding to 50% failure probability vs. defect size (the so-called Kitagawa-Takahashi diagram). The subsequent SEM observation of micro-notched run-out specimens has revealed the presence of non-propagating cracks at the tip of the micro-notches. This is in agreement with Murakami's concepts [22] for which the fatigue limit in presence of defects corresponds to the threshold condition of non-propagating cracks emanating from the defects themselves (that can then be treated as small cracks).

Fatigue limit data could be interpolated (Fig. 2a) by a relationship [23] originally proposed by El-Haddad [20] but expressed in terms of Murakami's √area parameter:

$$\sigma_w = \sigma_{wo} \cdot \sqrt{\frac{\sqrt{area_o}}{\sqrt{area} + \sqrt{area_o}}} \qquad (1)$$

where σ_{wo} is the fatigue limit amplitude for smooth specimens and $\sqrt{area_o}$ is the "El-Haddad" parameter (in particular $\sqrt{area_o}$ obtained by fitting data is 270 μm).

It is finally worth noting (Fig. 2a) that the design fatigue limit, proposed in the EN13103/4 standards [13-14] for solid axle bodies in A1N steel (equal to 166 MPa), corresponds to the stress

range of the non propagation of defects characterized by √area=400 μm. The estimated sizes of maximum corrosion defects on axles retired from service [17, 18] exceed this value: a design stress of 150 MPa should be adopted to ensure a non-propagation condition of surface defects detected in these axles.

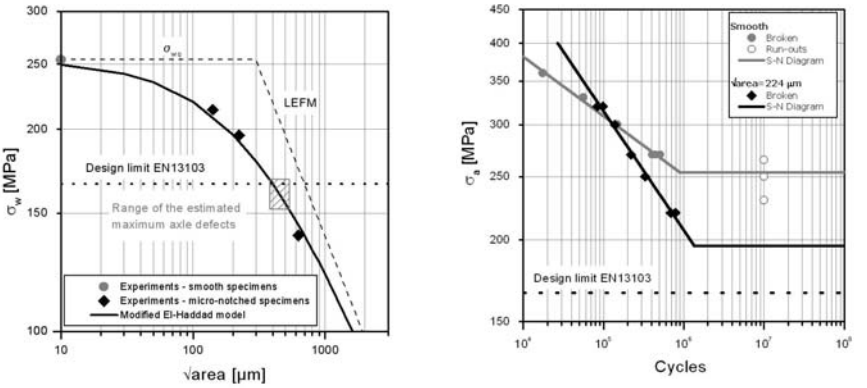

Fig. 2: Results of fatigue tests in air (R=-1): a) Kitagawa-Takahashi diagram in which, for comparison, is reported the range of the extimated maximum defects on axles retired from service [17, 18]; b) comparison of S-N diagrams for smooth and micro-notched (√area=224 μm) specimens.

S-N diagram S-N diagrams were experimentally derived for both a series of smooth and micro-notched specimens with a √area=224 μm. The specimens had the same shape and were prepared as previously described for fatigue limit tests. Tests were carried out by a four point rotating bending machine (capacity equal to 35 Nm) working at a frequency of approximately 10 Hz.

Experimental results are reported in Fig. 2b in terms of stress amplitudes σ_a corresponding to 50% failure probability. As it can be seen and expected, the presence of a defect significantly modifies, towards a shorter life, the slope of the S-N diagram. The same diagram also reports the lines corresponding to fatigue limit tests under axial loading. Recent analyses about corrosion defects detected on A1N axles retired from service [25] have shown that maximum corrosion defects can exceed this size.

Experiments in corrosive environment

In order to evaluate the reduction of A1N fatigue strength in corrosive environment, a series of corrosion fatigue tests were performed on smooth and micro-notched specimens (the latter again characterized by a √area=224 μm). These specimens had the same shape and were prepared as previously described for fatigue tests in laboratory air.

Laboratory accelerated tests In order to simulate the atmospheric aggressive environment effect on the fatigue strength of axles during laboratory accelerated fatigue tests, exposure of the specimens to cyclic wet/dry conditions and Cl- concentrated droppings, representing exposure to chlorides, was adopted [26].

Corrosion was applied to specimens by means of a dedicated experimental system based on the same four point rotating bending machine previously described and operating at 6÷8 Hz. This frequency value is representative of axles during a service speed equal to 60÷80 Km/h and allows the same interaction time between corrosive environment and stressed material to be reproduced in the laboratory. Each specimen was continuously subjected to wet/dry cycles (3h) consisting of a wet period (1h) followed by a dry period (2h). During the first 10 minutes of the dry period a hair-dryer

was used on the specimens, while artificial rainwater solution was provided, on the gage length, during the wet period by means of a dropping system. The artificial rainwater solution [27], characterised by pH=5, was produced as follows: ammonium sulphate 46.2 mg/dm^3, sodium sulphate 31.95 mg/dm^3, sodium nitrate 21.25 mg/dm^3 and sodium chloride 84.85 mg/dm^3. The chloride solution was a 0.9% NaCl solution made by using laboratory grade sodium chloride and de-ionized water. It was applied to specimens by an independent dropping system, only 10 minutes every 864000 cycles (corresponding to about once every 24h). Handling of corrosive environment was facilitated by the test configuration, presenting the specimen arranged horizontally.

Before performing corrosion fatigue tests, some micro-notched specimens were axially pre-cracked at R=-1 to a crack length equal to one of the micro-notches. This was done in order to compare fatigue test results obtained from both notched and cracked specimens. Tests carried out at low stress levels were often interrupted in order to remove rust, clean the specimen and examine it with the optical microscope.

Test results obtained from micro-notched specimens The S-N diagram obtained from micro-notched specimens is reported in Figure 3a. The data clearly show that: i) there is not a significant reduction of fatigue life for stress levels higher than σ_w; ii) some failures were observed for stress levels significantly lower than the in-air fatigue limit. This second observation suggests a significant reduction/disappearance of the in-air fatigue limit itself and, consequently, the possibility to have failures below the design limit [13]. This disappearance can be explained, for stress levels not sufficient to nucleate and propagate a crack in air conditions, by the simultaneous action of chemical and mechanical driving forces in terms of nucleation and environment-assisted crack growth [7-8, 28].

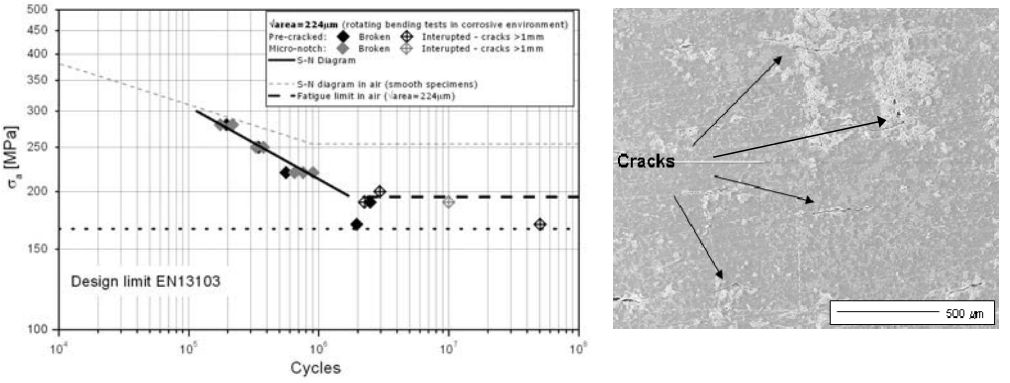

(a) (b)

Fig. 3: (a) S-N diagram for micro-notched and pre-cracked specimens in corrosive environment. (b) SEM analysis of specimen surface (tested at 170 MPa, broken at 1.97 MLN cycles).

It is also worth noting that no significant differences were observed in fatigue tests carried out on micro-notched or pre-cracked specimens. Furthermore, it appears that the pre-cracking does not play a key role in the failure process.

Broken and interrupted specimens were analysed and observed by SEM after the tests. It can be seen from the failure sections, that numerous cracks nucleated and propagated during the test, but the failure was finally caused by the "primary" crack. What is even more interesting is that, generally, the primary crack did not start from the micro-notch, which can be actually at the origin of a "secondary" crack. As shown in Fig. 3b for the specimen tested at 170 MPa and broken after 1.97 MLN cycles multiple cracks (evidenced by polishing, cleaning and slightly pulling the specimen under a tensile testing machine for breaking it are spread all over the surface of the

specimen and the failure started again not from the micro-notch, but elsewhere (the main fracture is outside the picture). Moreover, it should be noted that the growth of cracks from the pre-cracked micro-notches was observed at stress levels lower than the in-air threshold fatigue limit: this means that the presence of artificial rainwater reduces ΔK_{th} for A1N steel (as it has been observed by Ishihara et al. [26]).

The phenomena of multiple crack nucleation and failure outside the micro-notch were typically observed on specimens tested at low stresses (i.e. close to fatigue limit). In the case of high stresses, multiple cracks could be generally observed, but failures typically started from micro-notches. It is interesting to consider the competitive effect of corrosion cracking and surface corrosion by means of the other specimen tested at 170 MPa and interrupted after 50 MLN cycles. In this case, the evolution of the surface of the specimen was monitored. After 10 MLN cycles in wet/dry conditions, the pre-crack grew beyond the defect edge because of the corrosive environment (this crack without the corrosive effect should not propagate). After 20 MLN cycles, in the same conditions, the notch was partially eroded because of the surface generalized corrosion and after 50 MLN cycles the notch was totally eroded, and multiple cracks were present and spread all over the specimen surface. This evidence, together with the that shown in Fig. 3b, suggests the presence of a competitive mechanism of surface thinning (due to generalized corrosion) vs. the crack propagation from corrosion pits in the corrosion fatigue process of A1N steel in rainwater conditions.

Test results obtained from smooth specimens The experimental results obtained from smooth specimens are shown in Figure 4, where for comparison, also the S-N data for micronotched specimen (√area=224 μm) are reported.

Considering broken specimens, the slope of the curve is very similar to the one obtained in air.

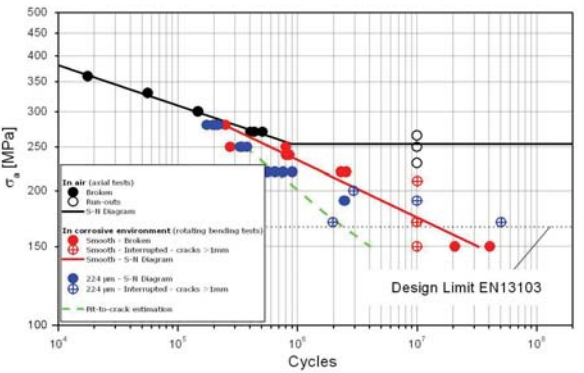

Fig. 4: S-N diagram for smooth specimens in corrosive environment (S-N data for micronotched specimen (√area=224 μm) are reported for comparison).

For stress levels below the fatigue limit (stress lower than 210 MPa), tests were interrupted at 10 MLN cycles and they displayed, after cleaning and slightly pulling the specimens, a strong surface damage very similar to the one shown in Fig. 3b. Because of this mechanism, micro-notched specimens failed outside the notch were treated as smooth specimens.

Eventually, two more specimens were tested at 150 MPa, which were let to run for more than 10 MLN cycles: they failed at 20 MLN and 50 MLN cycles, respectively. This evidences that: i) also the fatigue limit of smooth specimens seems to disappear in a corrosive environment; ii) the design limit proposed by EN13103 standard [13] does not seem to be conservative for corrosive environments.

Considering the BASS design limit (110 MPa), which is valid for steels with UTS of 550-650 MPa, the design fatigue life under constant amplitude stress and corrosion is 9.5 10^7 cycles, which corresponds to approx. 300,000 km for an axle.

On the other hand, one way of overcoming the design rules based on the fatigue limit stress is to calculate the fatigue damage experienced by the axle during service life [29]. From this point of view, it is important to observe that the S-N diagram in a corrosive environment shows a continuous decrease of the stress amplitude even in the case of a high number of cycles.

Pit-to-crack development

Some remarks can be added to what has already been observed and described. Fig. 5a shows a detail of the crack tip of a specimen subjected to fatigue in presence of corrosion. It is possible to see a very peculiar process zone characterised by a zig-zag pattern which is unusual for crack propagation in laboratory air.

The aspect ratio, in terms of crack depth, of a certain number of surface cracks observed on different specimens tested at different load levels is shown in Fig. 5b. In order to determine the depths of the cracks in question, all the fracture surfaces of broken specimens were observed with the SEM. As it can be seen, the morphology of the cracks is typically shallow. This shows corrosion assisted crack growth at the crack tip and suggests that crack growth rates are significantly enhanced by the environmental conditions.

The stress intensity factor of the same shallow cracks shown in Fig. 5b has been calculated, by Newman-Raju's solution [30], and compared with the Kitagawa-Takahashi diagram plotted in terms of threshold stress intensity factor (Fig. 5d). All the considered surface cracks presented a stress intensity factor lower than the diagram, so suggesting their non-propagation condition in the case of laboratory air environment. In corrosive environment, instead, corrosion assisted crack growth causes the disappearance of the fatigue limit and, consequently, the lowering of the ΔK_{th} values permitting further propagation and possible failure. In Fig. 5d is also reported the level of the effective threshold stress intensity factor $\Delta K_{th,eff}$ derived from special experiments in laboratory air described elsewhere [25]. Considering that small cracks were propagating and that the pit-to-crack transition had therefore already occurred [28, 31], the data clearly show that ΔK_{th} for fatigue propagation of small cracks in A1N in corrosive environment is lower than 1 MPa$\sqrt{m}$. This result implies that the effect of environmental conditions (i.e. environmentally assisted crack growth) can be very significant for the estimation of propagation life of axles under in-service conditions.

Fatigue crack growth (FCG, da/dN-ΔK curves) in corrosive environment are now running on precracked SE(B) specimens using a dedicated bench and artificial rainwater as corrosive environment. Comparison between S-N curve and FCG resistance curve of precracked specimens provide a good indication of the effect of the environment on fatigue crack initiation and propagation.

In particular, if a crack progated from a pit and having a depth of 100 μm ($\sqrt{area}$= 140 μm) is considered (Fig. 5d), the da/dN curve in corrosive environment allow us to estimate the pit-to-crack transition as reported in Fig. 4.

Conclusions

Corrosion fatigue is an important topic in the evaluation of railway axles' structural integrity since some recent axle failures have been attributed to the presence of corrosion pits or corrosion of the axle surface. In the current paper, the effect of corrosion upon fatigue properties of A1N steel were studied in order to assess the detrimental effects of corrosion and corrosion-fatigue in the presence of a mildly corrosive substance like rainwater.

The first part of the research was dedicated to the analysis of the influence of defects on fatigue strength of A1N steel in air. The results of this analysis showed that the size of extreme surface defects are relevant since, if they are treated as small mechanical cracks, they significantly reduce the fatigue strength to levels below the design limit of existing EN standards.

The second part of this research paper was devoted to conducting rotating bending fatigue experiments on smooth specimens both in the presence of artificial rainwater with a pH = 5 and in the presence of small mechanical cracks. The results showed that corrosion-fatigue enhances the growth of small cracks and continuously lowers the fatigue strength of A1N steel. According to these experimental results if the design fatigue limit of 110 MPa suggested in BASS 503/4 is considered, the ensured corrosion fatigue life corresponds to 300.000 km for an axle.

Also, the pit-to-crack transition has then been analysed and the results show that ΔK_{th} for fatigue propagation of small cracks in A1N in corrosive environment is lower than 1 MPa$\sqrt{m}$.

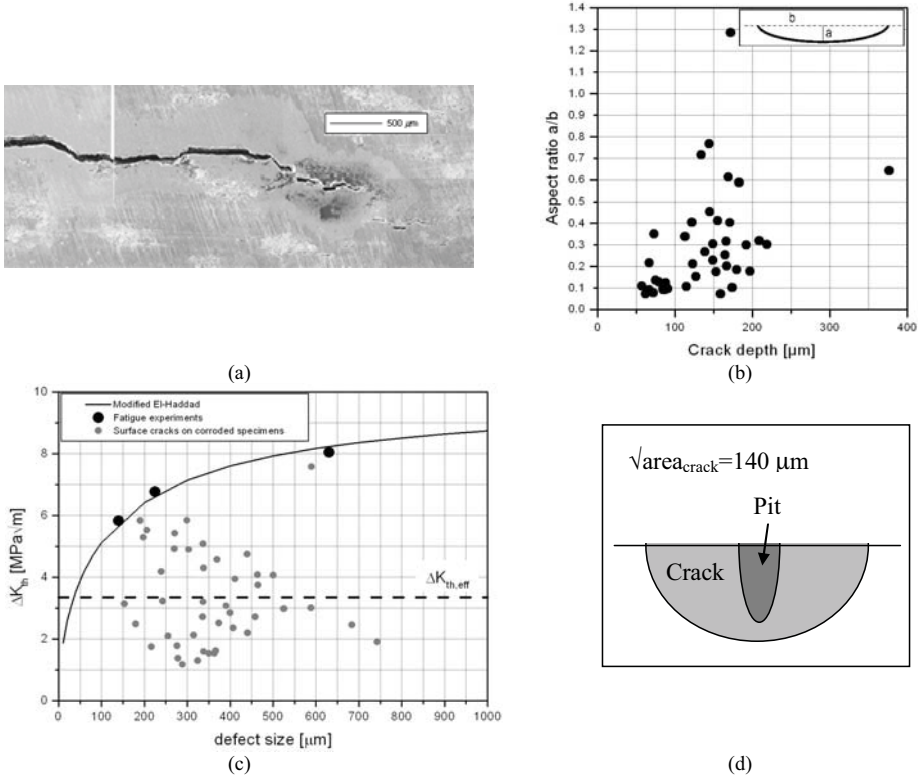

Fig. 5: Some aspects of corrosion damage and cracks: a) local damage phenomenon at the tip of a dominant crack; b) aspect ratio of cracks observed on tested specimens; c) Kitagawa-Takahashi diagram plotted in terms of threshold stress intensity factor, d) defect size for the estimation of the pit-to-crack transition.

References

[1] Snell, J.R.: J. Rail and Rapid Transit, 218, 2004, 279.

[2] Beretta, S. et al.: Eng. Fract. Mech., 72, 2005, 195.

[3] Zerbst, U. et al.: Eng. Fract. Mech., 72, 2005, 209.

[4] WIDEM EU Project. Wheelset Integrated Design and Effective Maintenance:www.widem.org.

[5] Hoddinot, D.S.: J. Rail and Rapid Transit, 218, 2004, 283.

[6] Transportation Safety Board of Canada: Railway Investigation Report R01Q0010, 2001.

[7] Schijve, J.: Fatigue of Structures and Materials. Kluwer Academic Publishers, New York, USA, 2004.

[8] Akid, R. et al.: Fatigue Fract. Engng Mater. Struct., 14, 1991, 637.

[9] Miller, K.J.: Mat. Science Tech., 9, 1993, 453.

[10] Ragab, A. et al.: Fatigue Fract. Engng Mater. Struct., 12, 1989, 469.

[11] **BR BASS 503.** Design guide for the calculation of stresses in driving axles. Railway Companies of 1996, Issue C, 1996.

[12] **BR BASS 504.** Design guide for the calculation of stresses in non-driving axles. Railway Companies of 1996, Issue C, 1996.

[13] **EN13103.** Railway Applications- Wheelsets and Bogies – Non Powered Axles – Design Method. CEN, 2001.

[14] **EN13104.** Railway Applications- Wheelsets and Bogies – Powered Axles – Design Method. CEN, 2001.

[15] **ERRI Question B136 Report n.** 11, Wheelset with assembled axleboxes: design, maintenance and standardisation, 1979.

[16] **BS EN13261.** Railway Applications- Wheelsets and Bogies –Axles – Product Requirements. CEN, 2003.

[17] Beretta S. et al., (2007), Impact of corrosion upon fatigue properties of A1N steel, Proc. 15th Int. Wheelset Congress, Prague, Czech Republic.

[18] Beretta S. et al. (2007) An investigation of the effects of corrosion on the fatigue strength of A1N steel railway axles, accepted for publication on Journal of Rail and Rapid Transit.

[19] BS EN13261. CEN, 2003.

[20] Beretta, S. et al.: J. Rail and Rapid Transit, 218, 2004, 317.

[21] Kitagawa, H. et al.: In: Proceedings of the 2nd International Conference on Mechanical Behaviour of Materials, 1976.

[22] Murakami, Y. Metal Fatigue: Effects of Small Defects and Nonmetallic Inclusions. Elsevier, Oxford, 2002.

[23] Beretta, S.: In: Proc. of the 14th European Conference on Fracture, Krakow, Poland, 2002.

[24] El-Haddad, M.H. et al.: J. Eng. Mater. Tech., ASME Trans. 101, 1979, 42.

[25] Beretta et al.: Eng. Fract. Mech, 73, 2006, 2627.

[26] Chen Y.Y. et al.: Corrosion Science, 47, 2005, 1001.

[27] Brunoro, G. et al.: Corrosion Science, 45, 2003, 2219.

[28] Ishihara, S. et al.: Fatigue Fract. Engng Mater. Struct., 29, 2006, 472.

[29] Fisher, G. et al.: Bericht FB-226, LBF, Darmstadt, 2005.

[30] Newman, J. C. et al.: Engng. Frac. Mech., 15, 1981, 185.

[31] Zhou, S. et al.: Fatigue Fract. Engng Mater. Struct., 22, 1999, 1083.